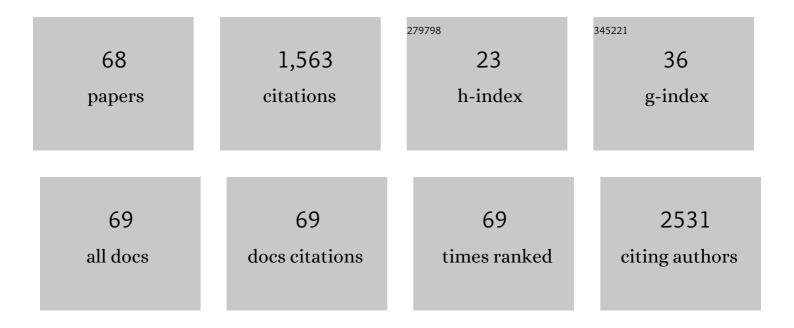
List of Publications by Year in descending order

Source: https://exaly.com/author-pdf/5033366/publications.pdf Version: 2024-02-01



IDI HENVCH

#	Article	IF	CITATIONS
1	Design Control of Copper-Doped Titania–Zirconia Catalysts for Methanol Decomposition and Total Oxidation of Ethyl Acetate. Symmetry, 2022, 14, 751.	2.2	3
2	Degradation of parathion methyl by reactive sorption on the cerium oxide surface: The effect of solvent on the degradation efficiency. Arabian Journal of Chemistry, 2022, 15, 103852.	4.9	3
3	Effect of crystal structure on nanofiber morphology and chemical modification; design of CeO2/PVDF membrane. Polymer Testing, 2022, 110, 107568.	4.8	6
4	Nickel-Decorated Mesoporous Iron–Cerium Mixed Oxides: Microstructure and Catalytic Activity in Methanol Decomposition. ACS Applied Materials & Interfaces, 2022, 14, 873-890.	8.0	5
5	Photocatalytic degradation of ciprofloxacin in water at nano-ZnO prepared by pulse alternating current electrochemical synthesis. Journal of Water Process Engineering, 2021, 40, 101809.	5.6	28
6	Size and nitrogen inhomogeneity in detonation and laser synthesized primary nanodiamond particles revealed via salt-assisted deaggregation. Carbon, 2021, 171, 230-239.	10.3	17
7	Formation of Catalytic Active Sites in Hydrothermally Obtained Binary Ceria–Iron Oxides: Composition and Preparation Effects. ACS Applied Materials & Interfaces, 2021, 13, 1838-1852.	8.0	11
8	Enhanced visible-light photodegradation of fluoroquinolone-based antibiotics and <i>E. coli</i> growth inhibition using Ag–TiO <sub>2</sub> nanoparticles. RSC Advances, 2021, 11, 13980-13991.	3.6	26
9	Nanostructured manganese oxides as highly active catalysts for enhanced hydrolysis of bis(4-nitrophenyl)phosphate and catalytic decomposition of methanol. Catalysis Science and Technology, 2021, 11, 1766-1779.	4.1	11
10	Size Effects on Surface Chemistry and Raman Spectra of Sub-5 nm Oxidized High-Pressure High-Temperature and Detonation Nanodiamonds. Journal of Physical Chemistry C, 2021, 125, 5647-5669.	3.1	25
11	Graphene Oxide Normal (GO + Mn2+) and Ultrapure: Short-Term Impact on Selected Antioxidant Stress Markers and Cytokines in NHDF and A549 Cell Lines. Antioxidants, 2021, 10, 765.	5.1	5
12	Anthropogenic records in a fluvial depositional system: The Odra River along The Czech-Polish border. Anthropocene, 2021, 34, 100286.	3.3	5
13	Bifunctional TiO2/CeO2 reactive adsorbent/photocatalyst for degradation of bis-p-nitrophenyl phosphate and CWAs. Chemical Engineering Journal, 2021, 414, 128822.	12.7	22
14	Crucial cytotoxic and antimicrobial activity changes driven by amount of doped silver in biocompatible carbon nitride nanosheets. Colloids and Surfaces B: Biointerfaces, 2021, 202, 111680.	5.0	6
15	Laser-Induced Modification of Hydrogenated Detonation Nanodiamonds in Ethanol. Nanomaterials, 2021, 11, 2251.	4.1	3
16	Nanocrystalline cerium oxide for catalytic degradation of paraoxon methyl: Influence of CeO2 surface properties. Journal of Environmental Chemical Engineering, 2021, 9, 106229.	6.7	15
17	Amidoxime-functionalized bead cellulose for the decomposition of highly toxic organophosphates. RSC Advances, 2021, 11, 17976-17984.	3.6	1
18	Novel synthesis of Ag@AgCl/ZnO by different radiation sources including radioactive isotope 60Co: Physicochemical and antimicrobial study. Applied Surface Science, 2020, 529, 147098.	6.1	9

#	Article	IF	CITATIONS
19	Mesoporous copper-ceria-titania ternary oxides as catalysts for environmental protection: Impact of Ce/Ti ratio and preparation procedure. Applied Catalysis A: General, 2020, 595, 117487.	4.3	8
20	Design and Performance of Novel Self-Cleaning g-C3N4/PMMA/PUR Membranes. Polymers, 2020, 12, 850.	4.5	14
21	Room-temperature synthesis of nanoceria for degradation of organophosphate pesticides and its regeneration and reuse. RSC Advances, 2020, 10, 14441-14450.	3.6	16
22	Synthesis and characterization of TiO <sub>2</sub> /Mg(OH) <sub>2</sub> composites for catalytic degradation of CWA surrogates. RSC Advances, 2020, 10, 19542-19552.	3.6	10
23	Reactive adsorption and photodegradation of soman and dimethyl methylphosphonate on TiO2/nanodiamond composites. Applied Catalysis B: Environmental, 2019, 259, 118097.	20.2	32
24	Solar light decomposition of warfare agent simulant DMMP on TiO2/graphene oxide nanocomposites. Catalysis Science and Technology, 2019, 9, 1816-1824.	4.1	13
25	Graphene oxide and graphitic carbon nitride nanocomposites assembled by electrostatic attraction forces: Synthesis and characterization. Materials Chemistry and Physics, 2019, 228, 228-236.	4.0	18
26	Can cerium oxide serve as a phosphodiesterase-mimetic nanozyme?. Environmental Science: Nano, 2019, 6, 3684-3698.	4.3	25
27	Mesoporous cerium oxide for fast degradation of aryl organophosphate flame retardant triphenyl phosphate. RSC Advances, 2019, 9, 32058-32065.	3.6	17
28	Structure and catalytic activity of hydrothermally obtained titanium-tin binary oxides for sustainable environment: Evaluation and control. Microporous and Mesoporous Materials, 2019, 276, 223-231.	4.4	6
29	Reactive adsorption of toxic organophosphates parathion methyl and DMMP on nanostructured Ti/Ce oxides and their composites. Arabian Journal of Chemistry, 2019, 12, 4258-4269.	4.9	28
30	Titania and zirconia binary oxides as catalysts for total oxidation of ethyl acetate and methanol decomposition. Journal of Environmental Chemical Engineering, 2018, 6, 2540-2550.	6.7	6
31	Chemical warfare agent simulant DMMP reactive adsorption on TiO2/graphene oxide composites prepared via titanium peroxo-complex or urea precipitation. Journal of Hazardous Materials, 2018, 359, 482-490.	12.4	23
32	Template-assisted hydrothermally obtained titania-ceria composites and their application as catalysts in ethyl acetate oxidation and methanol decomposition with a potential for sustainable environment protection. Applied Surface Science, 2017, 396, 1289-1302.	6.1	19
33	Water-based synthesis of TiO2/CeO2 composites supported on plasma-treated montmorillonite for parathion methyl degradation. Applied Clay Science, 2017, 144, 26-35.	5.2	14
34	Nanocrystalline cerium oxide prepared from a carbonate precursor and its ability to breakdown biologically relevant organophosphates. Environmental Science: Nano, 2017, 4, 1283-1293.	4.3	34
35	Graphene oxide/MnO 2 nanocomposite as destructive adsorbent of nerve-agent simulants in aqueous media. Applied Surface Science, 2017, 412, 19-28.	6.1	25
36	Fast and Straightforward Synthesis of Luminescent Titanium(IV) Dioxide Quantum Dots. Journal of Nanomaterials, 2017, 2017, 1-9.	2.7	3

#	Article	IF	CITATIONS
37	h-BN-TiO <sub>2</sub> Nanocomposite for Photocatalytic Applications. Journal of Nanomaterials, 2016, 2016, 1-12.	2.7	28
38	Photocatalytic and electrochemical properties of single- and multi-layer sub-stoichiometric titanium oxide coatings prepared by atmospheric plasma spraying. Journal of Advanced Ceramics, 2016, 5, 126-136.	17.4	13
39	Template-assisted hydrothermally synthesized iron-titanium binary oxides and their application as catalysts for ethyl acetate oxidation. Applied Catalysis A: General, 2016, 528, 24-35.	4.3	13
40	Mesoporous TiO2 powders as host matrices for iron nanoparticles. Effect of the preparation procedure and doping with Hf. Nano Structures Nano Objects, 2016, 7, 56-63.	3.5	12
41	Shape-controlled synthesis of Sn-doped CuO nanoparticles for catalytic degradation of Rhodamine B. Journal of Colloid and Interface Science, 2016, 481, 28-38.	9.4	45
42	Iron modified titanium–hafnium binary oxides as catalysts in total oxidation of ethyl acetate. Catalysis Communications, 2016, 81, 14-19.	3.3	12
43	Chemical mechanical glass polishing with cerium oxide: Effect of selected physico-chemical characteristics on polishing efficiency. Wear, 2016, 362-363, 114-120.	3.1	71
44	Accelerated dephosphorylation of adenosine phosphates and related compounds in the presence of nanocrystalline cerium oxide. Environmental Science: Nano, 2016, 3, 847-856.	4.3	28
45	Mesoporous manganese oxide for the degradation of organophosphates pesticides. Journal of Materials Science, 2016, 51, 2634-2642.	3.7	31
46	Cerium oxide for the destruction of chemical warfare agents: A comparison of synthetic routes. Journal of Hazardous Materials, 2016, 304, 259-268.	12.4	54
47	Nanostructured Metal Oxides for Stoichiometric Degradation of Chemical Warfare Agents. Reviews of Environmental Contamination and Toxicology, 2016, 236, 239-258.	1.3	10
48	Recovery of Cerium Dioxide from Spent Glass-Polishing Slurry and Its Utilization as a Reactive Sorbent for Fast Degradation of Toxic Organophosphates. Advances in Materials Science and Engineering, 2015, 2015, 1-8.	1.8	24
49	Graphene oxide nanoparticle attachment and its toxicity on living lung epithelial cells. RSC Advances, 2015, 5, 59447-59457.	3.6	9
50	Effect of preparation procedure on the formation of nanostructured ceria–zirconia mixed oxide catalysts for ethyl acetate oxidation: Homogeneous precipitation with urea vs template-assisted hydrothermal synthesis. Applied Catalysis A: General, 2015, 502, 418-432.	4.3	56
51	Degradation of organophosphorus pesticide parathion methyl on nanostructured titania-iron mixed oxides. Applied Surface Science, 2015, 344, 9-16.	6.1	35
52	Multi-component titanium–copper–cobalt- and niobium nanostructured oxides as catalysts for ethyl acetate oxidation. Reaction Kinetics, Mechanisms and Catalysis, 2015, 116, 397-408.	1.7	1
53	Chemical degradation of trimethyl phosphate as surrogate for organo-phosporus pesticides on nanostructured metal oxides. Materials Research Bulletin, 2015, 61, 259-269.	5.2	11
54	Magnetically separable reactive sorbent based on the CeO2/Î <sup>3</sup> -Fe2O3 composite and its utilization for rapid degradation of the organophosphate pesticide parathion methyl and certain nerve agents. Chemical Engineering Journal, 2015, 262, 747-755.	12.7	55

#	Article	IF	CITATIONS
55	<i>In Situ </i> <scp>FTIR</scp> Spectroscopy Study of the Photodegradation of Acetaldehyde and azo Dye Photobleaching on Bismuthâ€Modified TiO <sub>2</sub> . Photochemistry and Photobiology, 2015, 91, 48-58.	2.5	6
56	A green method of graphene preparation in an alkaline environment. Ultrasonics Sonochemistry, 2015, 24, 65-71.	8.2	24
57	ZnO/Bi2O3 nanowire composites as a new family of photocatalysts. Powder Technology, 2015, 270, 83-91.	4.2	18
58	Improvement of Orange II Photobleaching by Moderate Ga3+Doping of Titania and Detrimental Effect of Structural Disorder on Ga Overloading. Journal of Nanomaterials, 2014, 2014, 1-11.	2.7	2
59	Self-Assembled BN and BCN Quantum Dots Obtained from High Intensity Ultrasound Exfoliated Nanosheets. Science of Advanced Materials, 2014, 6, 1106-1116.	0.7	42
60	Photocatalytic oxidation of butane by titania after reductive annealing. Journal of Materials Science, 2014, 49, 4161-4170.	3.7	6
61	Role of bismuth in nano-structured doped TiO2 photocatalyst prepared by environmentally benign soft synthesis. Journal of Materials Science, 2014, 49, 3560-3571.	3.7	11
62	Ultrasound exfoliation of inorganic analogues of graphene. Nanoscale Research Letters, 2014, 9, 167.	5.7	58
63	Blue and green luminescence of reduced graphene oxide quantum dots. Carbon, 2013, 63, 537-546.	10.3	66
64	Doping of <scp><scp>TiO</scp></scp> <sub>2</sub> – <scp><scp>GO</scp></scp> and <scp><scp>TiO</scp></scp> <sub>2</sub> –r <scp>CO</scp> with Noble Metals: Synthesis, Characterization and Photocatalytic Performance for Azo Dye Discoloration. Photochemistry and Photobiology, 2013, 89, 1038-1046.	2.5	31
65	Feasible Synthesis of TiO <sub>2</sub> Deposited on Kaolin for Photocatalytic Applications. Clays and Clay Minerals, 2013, 61, 165-176.	1.3	13
66	Strongly luminescent monolayered MoS2 prepared by effective ultrasound exfoliation. Nanoscale, 2013, 5, 3387.	5.6	231
67	Impact of Ge <sup>4+</sup> Ion as Structural Dopant of Ti <sup>4+</sup> in Anatase: Crystallographic Translation, Photocatalytic Behavior, and Efficiency under UV and VIS Irradiation. Journal of Nanomaterials, 2012, 2012, 1-11.	2.7	8
68	Hydrogen peroxide route to Sn-doped titania photocatalysts. Chemistry Central Journal, 2012, 6, 113.	2.6	27